applied sciences

MDPI

Article

O_2 Loaded Germanosilicate Optical Fibers: Experimental In Situ Investigation and Ab Initio Simulation Study of GLPC Evolution under Irradiation

Imene Reghioua [1], Luigi Giacomazzi [2,3,*], Antonino Alessi [4], Blaz Winkler [2], Layla Martin-Samos [3], Sylvain Girard [1], Diego Di Francesca [1,5], Mattia Fanetti [2], Nicolas Richard [6], Philippe Paillet [6], Melanie Raine [6], Simonpietro Agnello [7], Matjaz Valant [2], Aziz Boukenter [1] and Youcef Ouerdane [1]

1 Laboratoire Hubert Curien, UMR CNRS 5516, Université Jean Monnet, F-42000 Saint-Etienne, France; imene.reghioua@cea.fr (I.R.); sylvain.girard@univ-st-etienne.fr (S.G.); diego.di.francesca@cern.ch (D.D.F.); aziz.boukenter@univ-st-etienne.fr (A.B.); ouerdane@univ-st-etienne.fr (Y.O.)
2 Materials Research Laboratory, University of Nova Gorica, Vipavska 11c, SI-5270 Ajdovscina, Slovenia; blaz.winkler@gmail.com (B.W.); mattia.fanetti@ung.si (M.F.); matjaz.valant@ung.si (M.V.)
3 Institute of Materials (IOM), National Research Council of Italy (CNR), c/o SISSA Via Bonomea 265, IT-34136 Trieste, Italy; marsamos@iom.cnr.it
4 Laboratoire des Solides Irradiés (LSI), UMR 7642 CEA-CNRS, Ecole Polytechnique, Route de Saclay, F-91128 Palaiseau, France; antonino.alessi@polytechnique.edu
5 European Organization for Nuclear Research (CERN), CH-1217 Meyrin, Switzerland
6 Direction des Applications Militaires (DAM-DIF), Commissariat à l'Energie Atomique (CEA), Bruyéres-le-Chatel, F-91297 Arpajon, France; nicolas.richard@cea.fr (N.R.); philippe.paillet@cea.fr (P.P.); melanie.raine@cea.fr (M.R.)
7 Dipartimento di Fisica e Chimica Emilio Segre', Università di Palermo, Via Archirafi 36, IT-90123 Palermo, Italy; simonpietro.agnello@unipa.it
* Correspondence: giacomazzi@iom.cnr.it

Abstract: In this work we present a combined experimental and ab initio simulation investigation concerning the Germanium Lone Pair Center (GLPC), its interaction with molecular oxygen (O_2), and evolution under irradiation. First, O_2 loading has been applied here to Ge-doped optical fibers to reduce the concentration of GLPC point defects. Next, by means of cathodoluminescence in situ experiments, we found evidence that the 10 keV electron irradiation of the treated optical fibers induces the generation of GLPC centers, while in nonloaded optical fibers, the irradiation causes the bleaching of the pre-existing GLPC. Ab initio calculations were performed to investigate the reaction of the GLPC with molecular oxygen. Such investigations suggested the stability of the dioxagermirane (DIOG) bulk defect, and its back conversion into GLPC with a local release of O_2 under irradiation. Furthermore, it is also inferred that a remarkable portion of the O_2 passivated GLPC may form Ge tetrahedra connected to peroxy bridges. Such structures may have a larger resistance to the irradiation and not be back converted into GLPC.

Keywords: optical fiber; O_2 loading; point defects

Citation: Reghioua, I.; Giacomazzi, L.; Alessi, A.; Winkler, B.; Martin-Samos, L.; Girard, S.; Di Francesca, D.; Fanetti, M.; Richard, N.; Paillet, P.; et al. O_2 Loaded Germanosilicate Optical Fibers: Experimental In Situ Investigation and Ab Initio Simulation Study of GLPC Evolution under Irradiation. *Appl. Sci.* **2022**, *12*, 3916. https://doi.org/10.3390/app12083916

Academic Editors: Nuno Silva and Nunzio Cennamo

Received: 30 November 2021
Accepted: 11 April 2022
Published: 13 April 2022

1. Introduction

Point defects in silica have attracted the attention of many research groups in the past few decades [1–8]. They cause the appearance of absorption bands in the glass transmission window [1–3], and consequently, defect generation or conversion implies variations of the optical properties of silica. It is well known that generation and conversion of point defects take place when silica is exposed to ionizing radiation, such as X- and γ-rays, as well as electron beams [1–8]. For these reasons, a relevant part of the study of radiation effects on silica-based optical fibers or bulk glasses has been devoted to point defect characterization in terms of electronic level structure, and identifying the absorption (sometimes luminescence) bands associated with each defect structure. At the same time,

the generation mechanisms and the conversion of defects were the main topics of a great number of investigations [3,8–16]. Moreover, a few experimental techniques, such as H_2 or O_2 loading of optical fibers, have been designed with the aim to enhance the radiation resistance by passivating radiation-induced point defects, and to enhance the duration of the optical fiber in a harsh environment [17,18].

One of the most important defects related to applicative and basic research relevance is the Germanium Lone Pair Center (GLPC [19]) in Ge-doped silica, which is employed to produce one of the most common optical fiber types in telecommunications and sensing applications [20,21]. It is accepted that the GLPC is an electron donor and that its presence affects the sensitivity of the silica to radiation or laser exposure [11,16,22]. The microscopic structure of such defect must be mentioned as well. The GLPC is a twofold coordinated Ge atom with two electrons forming a lone pair [19,23]. This defect is responsible for absorption bands at about 5.12 eV (related to a singlet–singlet transition) and at about 3.8 eV (related to a singlet–triplet transition) [19,23]. Furthermore, it is responsible for two emission bands at 4.3 eV (inverse singlet–singlet transition) and at ~3.1 eV (triplet–singlet transition, the triplet state can be populated by intersystem crossing processes) [19,23]. In particular, the latter emission at ~3.1 eV (i.e., ~400 nm) could be exploited to study the kinetics of creation or bleaching of GLPC centers in silica by means of cathodoluminescence (CL) spectroscopy [24,25].

In the present investigation, other aspects related to the GLPC must be remembered. The GLPC defect is usually present in high concentrations in nonirradiated optical fibers because of the manufacturing processes, and its concentration decreases when the fibers are exposed to radiation [26]. Furthermore, a recent investigation has proven that O_2 loading of the optical fiber is able to destroy these GLPC, then modify their response to consecutive irradiation [10], suggesting a possible method to tune the radiation response of germanosilicate optical fibers in the ultraviolet and visible domains. However, in this previous investigation, the basic mechanisms responsible for the GLPC bleaching in O_2 loaded fibers were not deeply investigated.

In this work, to better understand how O_2 loading bleaches the GLPC centers (before irradiation) and how they can be generated during irradiation in treated optical fibers, we completed our experimental work with ab initio calculations. These simulations enabled us to identify the relevant structures resulting from the reaction of the GLPC with molecular oxygen, and to evaluate the stability of such bulk defects and their possible back conversion to GLPC, or alternatively their permanent bleaching. In particular, the present work provides strong support in favor of the existence and stability of dioxagermirane (DIOG) as a bulk point defect in O_2-loaded Ge-doped fibers. The dioxagermirane defect is a germanium-based analogue of the dioxasilyrane [27], a point defect which was first detected as a surface defect on reactive silica [28] and has recently been found in luminescent siliceous materials and silica nanoparticles [29,30]. Moreover, in a previous theoretical study, the DIOG (i.e., the $(O_2)Ge=$ defect) was investigated as a surface defect in germanium oxides [31]. Although the DIOG still preserves the "memory" of the underlying defect (GLPC), we demonstrated that relaxation paths may exist which lead to a reconstruction of the tetrahedral network around the GLPC, resulting in a loss of memory of the original defect in O_2-loaded fibers. Since the O_2 molecule is one of the major diffusing species in silica, we have focused this work primarily on the formation of DIOG, which is likely to be the dominant mechanism for the GLPC bleaching during the O_2 loading process. The diffusion of atomic oxygen might lead, at a GLPC site, to the formation of germanone [10,32], which in principle could provide an alternative bleaching mechanism, is not considered hereafter. In fact, it requires the expensive dissociation of the O_2 molecule and the diffusion of atomic oxygen in silica, requiring activation energies above 1.3 eV, which is far less likely than the diffusion of molecular oxygen [33,34]. Though the formation of germanone might constitute a bleaching channel under extreme irradiation conditions, its study is beyond the scope of the present paper.

2. Materials and Methods

A two-step Ge-doped optical fiber produced by iXBlue Photonics Division [35] is studied in the present investigation. Such fiber has a total diameter of ~125 µm and a 62.5 µm core diameter. The inner part of the core has a diameter of ~40 µm and a Ge content of ~9 wt% (weight per cent), and such part is separated from the pure silica cladding by a ring made of 5 wt% Ge-doped silica, with a width of about 10 µm. The chemical composition of the investigated sample has been previously reported [24].

The O_2 loading of the sample was performed by keeping the sample in a PARR-4651 high pressure vessel at ~400 °C for ~21 days in a 90-bar oxygen atmosphere, according to previous investigation [10]. We stress that the presence of the O_2 inside such a treated fiber was tested by monitoring, as a function of the position along fiber diameters, the Raman line of the molecular oxygen [10,36]. Such studies proved that the content of O_2 is uniform along the fiber cross section with micrometer precision [10,36]. Independent experimental evidence of the effectiveness of our O_2-loaded treatment can also be inferred by the radiation-induced near-infrared luminescence of interstitial O_2, which is present in the loaded samples and absent in the untreated ones [37].

Cathodoluminescence and electron irradiation (at room temperature) were performed simultaneously using a field emission-scanning electronic microscope (SEM) JEOL JSM 7100f, equipped with a GATAN MONOCL4 detector (spectral range 300–750 nm, 1.7–4 eV). The electron beam is used both to excite the luminescence of point defects and simultaneously to irradiate the sample. For the present investigation, we acquired CL monochromatic images by monitoring the intensity of the incoming CL signal from the fiber at the wavelength of about 400 (±5) nm (i.e., 3.1 eV), then we extracted the luminescence profile as a function of the position from the center of the fiber (and of the number of scans, i.e., time). Based on previous studies, we are confident that the signal at 400 nm is due to the GLPC emission [24]. We employed the following parameters: electron energy 10 keV, a probe current of 4.2 nA, and an exposition time of about 20 s per scan. The investigated area was adapted to capture the core of the optical fiber, so the size of all the CL images is (~90 × 70) μm^2. We note that for acquiring CL spectra, the scanned area by the electron beam is much smaller to facilitate the response of only the selected zone. For the same experimental conditions (beam energy, probe current . . .), the dose rate of the CL spectra is much higher compared to the CL imaging, with a difference of about 1.7×10^7 Gy/s. To avoid large irradiation effects, we used CL imaging to evaluate the GLPC luminescence kinetics.

The electron penetration and the accumulated dose were evaluated by Geant4 [38], and the results are displayed in Figure 1. Particularly, the interaction volume depends on the energy of the primary electrons. For an energy E = 10 keV, the electrons could penetrate up to ~1.3 µm. According to the Monte Carlo simulations, the estimated dose rate for the recorded CL images using the above conditions is about 3.36×10^4 Gy/s.

The first principle calculations presented in this work are based on Density Functional Theory (DFT) and were performed using the Quantum-ESPRESSO (QE) package [39]. We have adopted local-density approximation (LDA) for describing the exchange-correlation functional, together with norm-conserving pseudopotentials. Wave functions are expanded on a basis of plane waves up to a kinetic cutoff of 80 Ry. The expansion is carried out at the sole Γ point of the Brillouin zone, as justified by the size of the adopted supercell and the large band gap of our silica-based system [15]. The relaxation of the DIOG and GLPC atomic structures has been achieved by using the Broyden–Fletcher–Goldfarb–Shanno algorithm [39] and by setting up a threshold of 0.0025 eV $Å^{-1}$ on the atomic forces. For the calculation of the reaction pathways and energy barriers along the minimum energy path (MEP), we adopted the climbing image nudged elastic band (CI-NEB) method, as implemented in the QE distribution. For each application of the NEB method, we used 11 configurations (NEB images). A threshold of 0.1 eV $Å^{-1}$ (on the norm of the force orthogonal to the path) was applied as criterion for the convergence of the MEP. We note

that only a small set of GLPC configurations [15] was employed for the present investigation, leading to a statistically limited analysis.

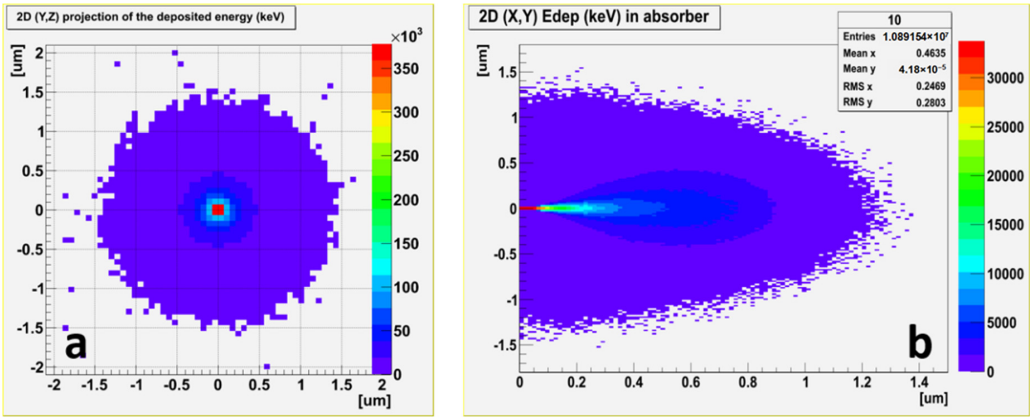

Figure 1. Geant4 simulation of the penetration depth and deposited energy distribution of 106 electrons (10 keV) in SiO_2. (**a**) (Y,Z) 2D cartography, (**b**) (X,Y) 2D cartography.

3. Results

3.1. In Situ CL Investigation of GLPC Kinetics in the O_2-Loaded Sample

In this section, we present experimental results of the CL in situ measurements. Figure 2 illustrates the normalized CL spectra of the Ge-doped optical fiber in the O_2-loaded and unloaded samples. We can easily observe that the luminescence at 400 nm is the main emission band in the core of both samples, and it is attributed (according to the literature) to the GLPC defects [24]. The normalized spectra are very similar and there is no change in the shape of the GLPC emission at 400 nm in the CL spectra, which indicates, at least from the spectroscopic point of view, that we are studying the same kind of centers.

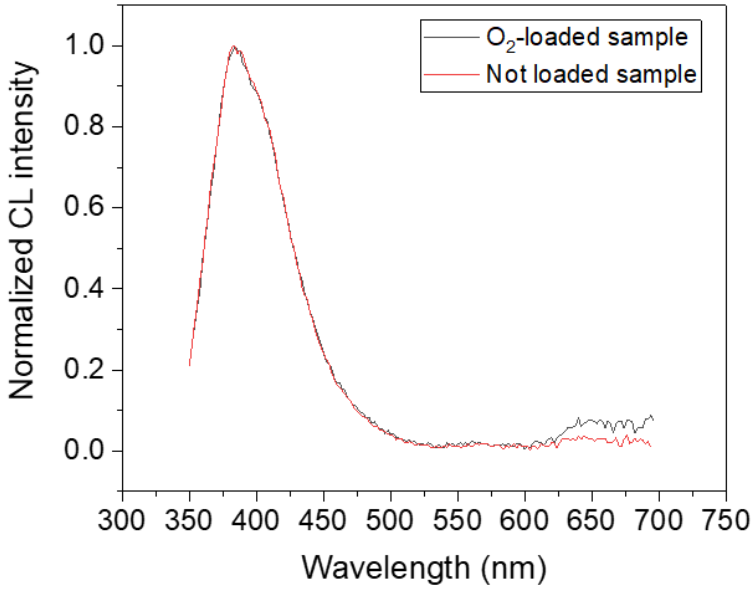

Figure 2. Normalized CL intensity taken in the center of the core of the Ge-doped optical fiber in the O_2-loaded and untreated samples.

We then followed on-line the kinetics of the emitting point defects using CL imaging. Many CL monochromatic images at 400 nm (±5 nm) were recorded as a function of the irradiation time up to ~30 min, then the luminescence profiles were extracted from these images following the method used previously [24]. In Figure 3 we present the

first (Figure 3a) and the last (Figure 3b) recorded monochromatic images of the sample. The different Ge-doped zones are distinguished by blue circles, where the central part is the one with ~9 wt% of Ge and the surrounding part is doped with ~5 wt% of Ge, as mentioned above.

Figure 3. CL monochromatic images acquired at 400 nm of the O_2 loaded fiber of (**a**) the first scanned image, (**b**) after 30 min of electron irradiation.

Comparing the two images, we can observe an increase of the luminescence signal after 30 min of irradiation. Moreover, the outer part seems to be brighter than the inner one. This indicates that the electron irradiation leads to an increase in the luminescence of the GLPC at 400 nm. In the first image, the CL signal is low since GLPC centers were bleached by the O_2-loading treatment as previously reported [10]. Such behavior differs from what is observed for nonloaded fibers [24], where the starting signal is high and is reduced by electron irradiation until it reaches a stable value [24]. With the aim of creating a better visualization of the above reported images, radial profiles were extracted following the method previously explained [24]. Figure 4a demonstrates the radial profiles of the first and the last CL monochromatic images, whereas Figure 4b presents the in situ kinetics of the GLPC luminescence as a function of the electron irradiation, which in this case is represented by the number of scans in the different Ge-doped regions.

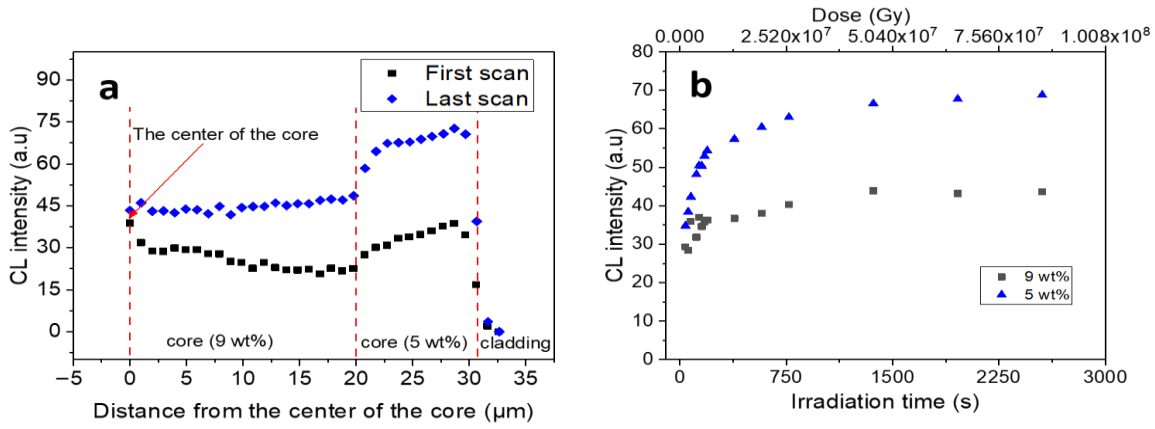

Figure 4. (**a**) Radial profiles of the first and the last recorded monochromatic CL images at 400 nm. (**b**) In situ kinetics of the GLPC CL at 400 nm as a function of the electron irradiation in the different Ge-doped zones. The estimated dose is 670 kGy per scan. In (**a**) vertical dashed lines are used to indicate the zoning of the fiber in terms of the core (Ge content of 9 and 5 wt%) and the cladding regions.

Basing on the results reported in Figure 4, we can notice that in the radial profile of the first scan, the intensity of the GLPC signal is slightly lower in the higher Ge-doped zone (i.e., for a distance from the center of the core < 20 µm). After 30 min of irradiation, the CL signal at 400 nm indicates an increase, which is still smaller in the higher Ge-doped region

than in the outer 5 wt% Ge-doped region. Following on line the kinetics in both zones (Figure 4b), we can observe that the increase in the GLPC signal is more efficient in the zone doped with 5 wt% as compared to the 9 wt% Ge-doped zone. Indeed, in the lower-doped zone, the signal increased by a factor of ~2. In our previous studies [24,40], we highlighted that the GLPC bleaching mechanism under electron irradiation of the untreated sample leads to an equilibrium state, where the remaining GLPC signal is also higher in the lower Ge-doped zone, even though it was not the case before irradiation. In Figure 5, we compare the radial profiles (normalized to the CL signal detected at about 15 µm from the core center) of the last recorded CL images of the O_2 loaded and the unloaded samples.

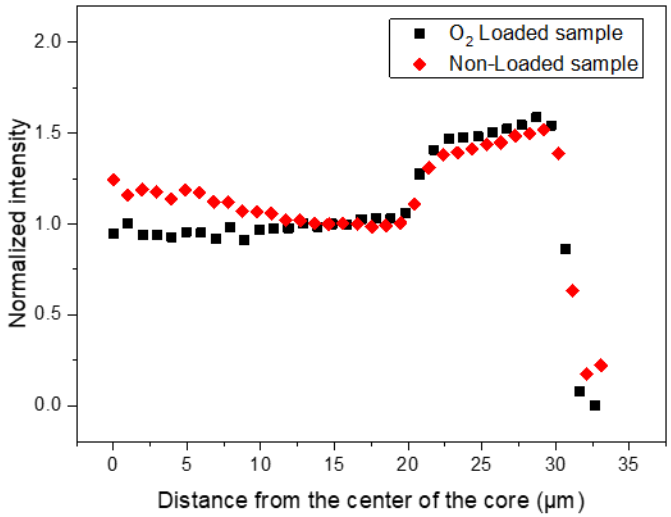

Figure 5. Normalized radial profiles, to the luminescence intensity detected at a distance of 15 µm from the core center, of the last recorded monochromatic images at 400 nm in the O_2-loaded sample (squares) and in the unloaded one (diamonds).

It isn't able that as the images of both samples were recorded separately, we normalized them to allow the comparison of their shapes. These normalized profiles are very close apart at the core center, where we note a difference within the 20% of the normalized signal. We conclude that whether the sample is O_2-loaded or not, the final normalized profile after electron irradiation is similar, with a higher GLPC signal in the lower-Ge-doped part. In this context, we emphasize that the same observation was reported previously [41], where pre-irradiated (γ-rays and UV) samples were investigated under electron irradiation, and their radial profiles after irradiation exhibit the same shape of the pristine one.

3.2. Ab Initio Calculations of Bulk Dioxagermirane Defects

To identify the relevant bleaching/creation mechanisms of GLPC point defects in O_2-loaded germanosilicate optical fibers, we have carried out a few dedicated first principle calculations. Since DIOG has been proposed as one of the possible defects involved in the oxygen-induced bleaching mechanisms of GLPC previously [10], we have obtained by first principle relaxation several DIOG point defects in a Ge-doped silica supercell model [15]. The DIOG structure involves an isosceles quasi-equilateral triangle OGeO, in which the two oxygen atoms of the O_2 molecule are bonded to the Ge of the GLPC, as schematically illustrated in Figure 6a.

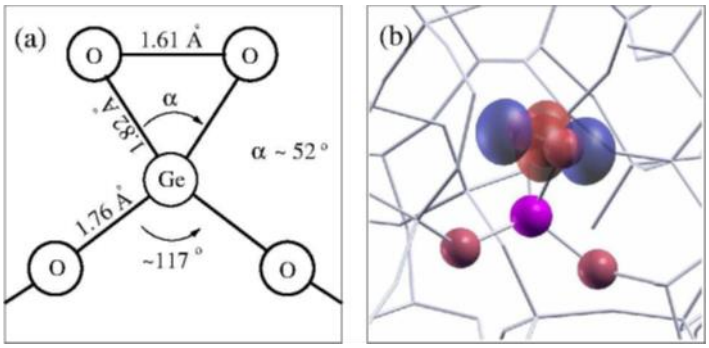

Figure 6. (**a**) Schematic representation of a dioxagermirane (DIOG): the angle α at Ge atom is expected to be of approximatively 52°. (**b**) Highest occupied molecular orbital (HOMO) of the DIOG configuration (shaded red and blue).

The molecular oxygen atoms form Ge–O bonds with an average Ge–O distance of 1.82 (±0.03) Å to be compared with the typical Ge–O bond distance (1.73–1.78 Å) in GeO_2 [42]. Furthermore, the O–O distance of 1.61 (±0.01) Å increases by about 30% with respect to the one of the free O_2 molecules (1.21 Å), resulting in a narrow O–Ge–O angle (Figure 6a) with mean value of 52.3° (±1.0°), in agreement with the geometric parameters reported previously [31]. Such a small angle involves considerably strained *p*-orbitals. Despite the likely stress on orbitals and consequent destabilization of the bonds, our calculations indicate that the DIOG configuration is a very robust bulk configuration, and 70% of our DIOGs could be properly relaxed with force convergence thresholds as small as those typically used (~0.0025 eV $Å^{-1}$) for vibrational spectra calculations [39,42]. The presence of a DIOG defect will cause the appearance of defect levels in the band gap of silica. In particular, the highest occupied molecular orbital (HOMO) level of a DIOG configuration is located ~2 eV above the top of the silica valence band, and it corresponds to *p*-orbitals of the O_2 oxygen atoms which are bonded to the GLPC (Figure 6b).

The formation energies of DIOG and GLPC centers have been calculated following the procedure outlined previously [15]. The calculated formation energy of the DIOG provides a mean value of ~4.5 eV, while the formation energy for a GLPC defect is ~0.6 eV larger. The latter discrepancy indicates that the absorption of an oxygen molecule at a GLPC site is a favorable process. This is understandable since the DIOG represents a step towards a healing path for the Ge-doped silica network, since it restores the fourfold coordination of the Ge atom. Overall, these results indicate that the dioxagermirane defects are good candidates for explaining the interaction of the excess oxygen with Ge lone pair defects (i.e., GLPC) in bulk silica. In fact, the latter interaction has been proven to annihilate a large portion of GLPC/ODC-II defects [10].

To better characterize the excess-oxygen absorption process at a GLPC, NEB simulations have been performed on Ge-doped silica to further evaluate if the absorption of an O_2 molecule at a GLPC site is a favorable process. Thus, silica configurations containing the DIOG defect and conversely the GLPC + O_2 configurations have been considered to be initial and final reaction configurations (Figure 7a,d). The calculated activation energies for the reaction of oxygen release from a DIOG defect span from 1.0 to 1.6 eV, with an average value of approximately 1.3 eV. Such an activation energy value falls in the upper bound of the range of activation energy values [~0.9 to 1.3 eV] reported in the literature for the migration of oxygen in silica [33,43,44]. The reverse reaction, which corresponds to the passivation of GLPC by an oxygen molecule (Figure 7), has an activation energy of approximately 0.2 eV, which further indicates that the absorption of an oxygen molecule is a favorable process.

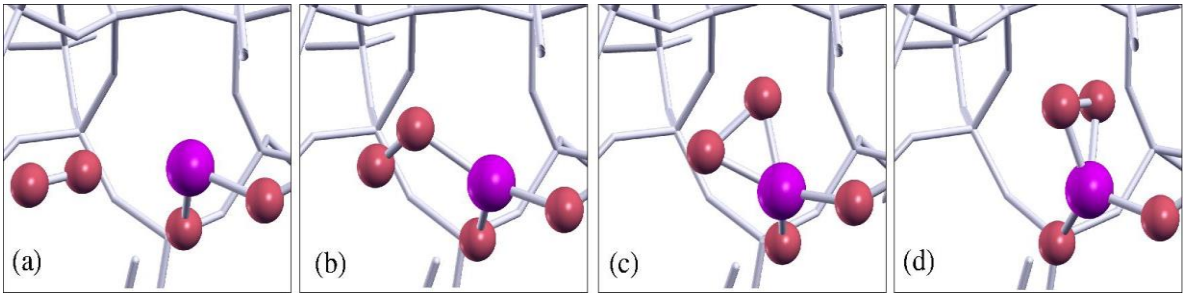

Figure 7. NEB snapshots illustrating the formation mechanism of a DIOG by passivating a GLPC with an O_2 molecule: (**a**) an O_2 molecule is placed at the center of a cavity nearby (about 3–5 Å) a GLPC, (**b**) The O_2 molecule binds to the GLPC, (**c**) a DIOG defect is formed, and (**d**) the DIOG structure is fully relaxed. O and Ge atoms of the DIOG are illustrated with red and purple balls, while for clarity, the rest of the network is illustrated with light grey sticks.

Besides the formation mechanism of DIOG in O_2 loaded Ge-doped silica fibers, we also have addressed the mechanism describing molecular oxygen interaction with GLPC and resulting in the reconstruction of the tetrahedron based network. A schematic representation of the reconstruction reaction can be seen in Figure 8. An oxygen atom from a nearby Si–O–Si bridge forms a bond with the Ge atom of the DIOG. At the same time, the DIOG moves closer to the Si–O–Si bridge so that the molecular oxygen attached to the Ge forms a new O–Si bond (with a temporarily fivefold-coordinated Si atom) and an O–Ge bond is broken. Finally, the structure relaxes into a GeO_4 tetrahedron connected to a peroxy bridge (having a O–O length of ~1.48 Å [45]). The likelihood of a network reconstruction mechanism following the interaction between O_2 molecule and GLPC is supported by the fact that a few NEB simulations of oxygen release from DIOG spontaneously provided it as an intermediate step. Moreover, in a few cases, DIOG could not be formed, or was temporarily formed, and the structural optimization directly resulted in a network reconstruction (i.e., the reconstruction reaction could happen spontaneously with no energy barrier). A detailed investigation of the network reconstruction reaction is however beyond the scope of the present paper and is not further discussed hereafter. Yet, our calculations allow us to speculate that the activation barrier is likely to be lower than ~1 eV, and thus it should be easily accessible with diffusion-based oxygen loading [10,15]. The comparison of formation energies between the reconstructed network configurations and their corresponding DIOG configurations indicates that the latter have a considerably larger (by ~1.2 eV) formation energy, indicating that the reconstruction of the network, whenever it occurs, represents the energetically favored endpoint.

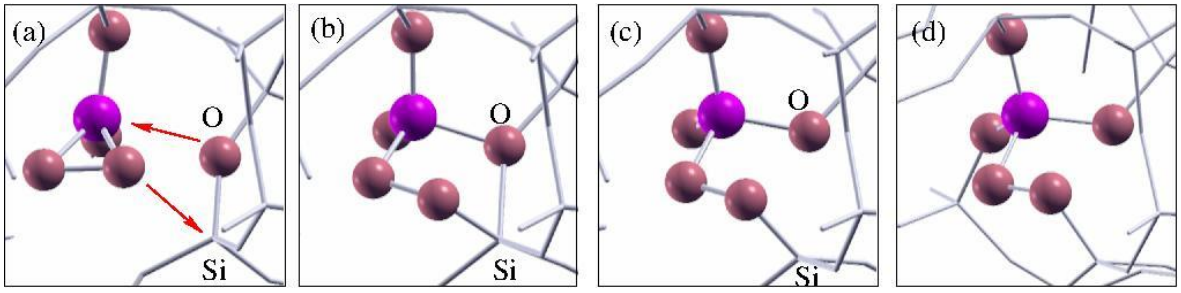

Figure 8. Schematic representation of the network reconstruction following the relaxation of a DIOG defect. (**a**) An oxygen atom of the network moves closer to a DIOG. (**b**) The O atom forms a bond with the Ge atom, temporarily becoming three-coordinated. (**c**,**d**) an O-Si bond is broken and the structure finally relaxes into a GeO_4 tetrahedron connected to a peroxy bond.

4. Discussion

As indicated by recent investigations, the O_2 loading of the optical fiber can destroy the GLPC centers and modify the optical fiber response to consecutive irradiation [10]. This is particularly interesting in the context of radiation-hardened optical fibers [17,18], particularly in the ultraviolet and visible domains. In the present work we provided strong evidence, in the O_2-loaded sample, of a GLPC increase (Figure 4) that is induced by electron irradiation. Such an increase is observed until the ~40th scan (dose ~2.7×10^7 Gy), then a limit value, confined within a factor ~2, is reached. The resulting behavior is similar in the two investigated Ge-doped regions (5 wt% and 9 wt%), even if the growth of the signal is higher in the less-doped parts of the fibers, while in the higher-doped region, a growth of only ~25% is recorded. We also note that due to the high dose rate in the first scan, each investigated point accumulates a dose of about 0.67 MGy. The observed behavior prompts two essential questions: what are the microscopic mechanisms behind the observed increase in the CL signal of GLPC centers, and what kind of point defects can arise from the interaction of an O_2 molecule with a GLPC in bulk silica?

Our ab initio results suggest that the O_2 loading of the optical fiber, which is performed prior to irradiation, can lead to the formation of bulk DIOG defects in silica. In fact, our calculations indicate that the DIOG could be readily formed whenever an oxygen molecule is present near the GLPC, i.e., in the presence of O_2 excess inside Ge-doped silica, thus providing an explanation for the bleaching effect of the O_2 loading on the GLPC concentration (Figure 3a). Under electron irradiation, some GLPC centers are regenerated due to the release of excited/ionized O_2 species from a DIOG (Figure 7). Particularly, the reaction in the case of neutral species requires overcoming an energy barrier (~1.3 eV), being easily accessible during irradiation [15,46], and representing an upper bound for the release of the excited/ionized O_2 species. Since O_2 at room temperature did not escape from the material, we approximated that (particularly when there is a starting excess of O_2 in the silica matrix) an equilibrium can be reached between the regeneration of GLPC under irradiation and the passivation by oxygen at room temperature which leads to the formation of dioxagermirane or other defects [10]. We note that electron-stimulated desorption may occur at the surface of samples as reported previously [47,48]. Specifically, oxygen might be desorbed, and because the sample volume is mostly occupied by silica, oxygen vacancies might be generated in silica, and ODC-II centers could be generated during the irradiation occasionally. Yet, since the CL measurements were carried out at room temperature, oxygen diffusion is low so that, regarding the GLPC center (and hence its luminescence), the effect of this surface desorption in the bulk is not relevant. DIOG could release molecular oxygen, but the latter would not move far from the GLPC, so we do not expect it to lead to a remarkable desorption from the sample at room temperature within the total irradiation time.

As the oxygen loading is often performed using diffusion mechanisms at temperatures around ~500 °C [10], it could be speculated that a combination of excess oxygen and temperature could reconstruct the network at a GLPC site, similar to an oxygen molecule easily passivating an oxygen vacancy and forming a peroxy defect. The reconstruction reaction at a GLPC site may be a more complex network relaxation, analogous to the GLPC generation from an oxygen (mono-)vacancy which involves advanced "rotation" and "puckering" mechanisms [15]. The mechanism displayed in Figure 8 may provide a way to completely remedy the structural memory of the preexisting GLPC defect at certain network sites, so that further irradiation treatments would not regenerate it, leading to a partial regeneration of GLPC in O_2-loaded samples. Furthermore, the latest experimental studies indicate that the oxygen is most probably incorporated into the network in the form of peroxy bridges [49].

Even if the CL experiment implies that the data of the first image is due to an irradiated sample, and even if a quantitative comparison of the final intensities detected in the O_2-loaded and unloaded fiber should be performed (however difficult), it is interesting to note that in both samples, a limit value is reached at a high dose (Figure 5). Consequently,

although a quantitative comparison of these two values needs further investigation, a stable amount of GLPC exists. Furthermore, we note that in one case (unloaded sample) we bleached and destroyed the GLPC centers, whereas in the other case, we generated them after the O_2 loading had significantly reduced their concentration before irradiation. It is also worth noting that both the normalized profiles reported in Figure 5 strongly suggest a role of the Ge content in determining such stable content, at least for the investigated values of 5 wt% and 9 wt%. The latter remark implies that suitable doping strategies may be envisaged to control the final amount of GLPC centers.

In summary, our investigation provides a strong support in favor of the formation and stability of DIOG bulk point defects in O_2-loaded Ge-doped fibers. Next, under electron irradiation, the DIOG can release molecular oxygen and convert back to GLPC, thus providing a reasonable explanation for the observed CL increase in GLPC intensity in irradiated samples (Figures 3 and 4). Furthermore, our calculations suggest that an important fraction of GLPC sites could be passivated permanently by O_2, resulting in the formation of a low-energy configuration which exhibits "healed" Ge tetrahedra linked to peroxy bridges (Figures 8 and 9). The latter configuration might not convert back to GLPC under irradiation, resulting in a lower final intensity of GLPC in O_2-loaded samples compared to the unloaded and nonirradiated one.

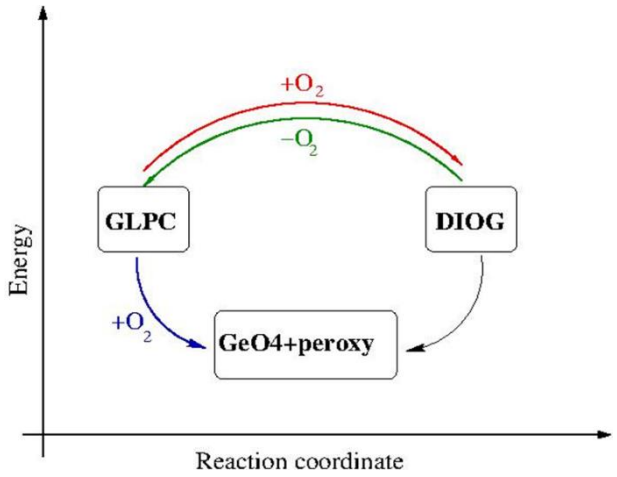

Figure 9. Schematic representation of the possible bleaching paths of GLPC in O_2-loaded optical fibers together with back conversion paths from DIOG as derived by ab initio calculations.

5. Conclusions

In this work, by means of cathodoluminescence experiments, we have demonstrated that electron irradiation of O_2-loaded Ge-doped optical fibers leads to the generation of GLPC centers, at variance with the behavior observed in unloaded optical fibers, where the irradiation causes bleaching of the GLPC. Moreover, by means of ab initio calculations, we have identified relevant structures resulting from the reaction of the GLPC center with molecular oxygen (i.e., the DIOG point defect, or alternatively, the complex formed by a healed GeO_4 tetrahedron connected to a peroxy bridge) and discussed how much such bulk defects are stable and can reform GLPC, or alternatively correspond to a permanent bleaching. Hence the present combined experimental and ab initio investigation allows us to interpret the generation of GLPC centers, in irradiated O_2-loaded germanosilicate fibers, in terms of oxygen-release reaction from DIOG bulk defects.

Author Contributions: Conceptualization, D.D.F., A.A., L.G., L.M.-S., I.R., B.W. and S.A.; methodology, L.M.-S., B.W., L.G., A.A. and D.D.F.; software, L.M.-S., B.W., L.G., N.R. and M.R.; formal analysis, I.R., M.R., B.W., L.G. and M.F.; investigation, I.R., B.W. and M.F.; resources, A.B., Y.O., S.G., L.M.-S., L.G., M.V. and M.F.; data curation, I.R. and B.W.; writing—review and editing, I.R., L.G., A.A., B.W., D.D.F., S.G., L.M.-S., M.F., N.R., P.P., M.R., S.A., M.V., A.B. and Y.O.; supervision, S.G., L.M.-S., A.B.

and Y.O.; funding acquisition, S.G., L.G., L.M.-S., M.V., N.R., P.P., A.B. and Y.O. All authors have read and agreed to the published version of the manuscript.

Funding: B.W. and L.M.-S. acknowledge support through the Young Researcher Grant from the Slovenian Research Agency (ARRS), 5100-12/2014-5, CEA/ARRS grant. L.G. and M.V. acknowledge support through CEA-ARRS bilateral grant number n. 00018 (As4DS) and ARRS research core funding n. P2-0412.

Data Availability Statement: The datasets generated during and/or analysed during the present study are available from the corresponding author under specific request.

Acknowledgments: We acknowledge support from CINECA for providing high performance computing resources (Project OXYRIS-HP10B5K2GU).

Conflicts of Interest: The authors declare no conflict of interest.

References

1. Skuja, L.; Hirano, M.; Hosono, H.; Kajihara, K. Defects in oxide glasses. *Phys. Stat. Sol. C* **2005**, *2*, 15–24. [CrossRef]
2. Girard, S.; Kuhnhenn, J.; Gusarov, A.; Brichard, B.; Van Uffelen, M.; Ouerdane, Y.; Boukenter, A.; Marcandella, C. Radiation Effects on Silica-Based Optical Fibers: Recent Advances and Future Challenges. *IEEE Trans. Nucl. Sci.* **2013**, *60*, 2015–2036. [CrossRef]
3. Pacchioni, G.; Skuja, L.; Griscom, D.L. *Defects in SiO_2 and Related Dielectrics: Science and Technology*; NATO Science Series II: Mathematics, Physics and Chemistry; Kluwer Academic: Dordrecht, The Netherlands, 2000.
4. Chiodini, N.; Meinardi, F.; Morazzoni, F.; Paleari, A.; Scotti, R. Optical transitions of paramagnetic Ge sites created by *X*-ray irradiation of oxygen-defect-free Ge-doped SiO_2 by the sol-gel method. *Phys. Rev. B* **1999**, *60*, 2429–2435. [CrossRef]
5. Kristensen, M. Ultraviolet-light-induced processes in germanium-doped silica. *Phys. Rev. B* **2001**, *64*, 144201. [CrossRef]
6. Takahashi, M.; Uchino, T.; Yoko, T. Correlation between Macro- and Microstructural Changes in Ge:SiO_2 and SiO_2 Glasses under Intense Ultraviolet Irradiation. *J. Am. Ceram. Soc.* **2002**, *85*, 1089–1092. [CrossRef]
7. Buscarino, G.; Agnello, S.; Gelardi, F.M.; Boscaino, R. Polyamorphic transformation induced by electron irradiation in *a*-SiO_2 glass. *Phys. Rev. B* **2009**, *80*, 94202. [CrossRef]
8. Alessi, A.; Agnello, S.; Gelardi, F.M. Properties and Generation by Irradiation of Germanium Point Defects in Ge-Doped Silica. In *Germanium: Properties, Production and Applications*; Germanno, R.V., Ed.; Nova Science Publishers: New York, NY, USA, 2012; pp. 75–150.
9. Griscom, D.L. Trapped-electron centers in pure and doped glassy silica: A review and synthesis. *J. Non-Cryst. Solids* **2011**, *357*, 1945–1962. [CrossRef]
10. Di Francesca, D.; Agnello, S.; Girard, S.; Alessi, A.; Marcandella, C.; Paillet, P.; Boukenter, A.; Gelardi, F.M.; Ouerdane, Y. O_2-Loading Treatment of Ge-Doped Silica Fibers: A Radiation Hardening Process. *J. Lightw. Technol.* **2016**, *34*, 2311–2316. [CrossRef]
11. Griscom, D.L. On the natures of radiation-induced point defects in GeO_2-SiO_2 glasses: Reevaluation of a 26-year-old ESR and optical data set. *Opt. Mat. Express* **2011**, *1*, 400–412. [CrossRef]
12. Griscom, D.L. Fractal kinetics of radiation-induced point-defect formation and decay in amorphous insulators: Application to color centers in silica-based optical fibers. *Phys. Rev. B* **2001**, *64*, 174201. [CrossRef]
13. Kashaykin, P.F.; Tomashuk, A.L.; Khopin, V.F.; Firstov, S.V.; Guryanov, A.N.; Dianov, E.M. Observation of radiation-induced absorption of self-trapped holes in Ge-doped silica fiber in near infrared range at reduced temperature. *J. Non-Cryst. Solids* **2018**, *496*, 24–28. [CrossRef]
14. Alessi, A.; Agnello, S.; Sporea, D.G.; Oproiu, C.; Brichard, B.; Gelardi, F.M. Formation of optically active oxygen deficient centers in Ge-doped SiO_2 by γ-and β-ray irradiation. *J. Non-Cryst. Solids* **2010**, *356*, 275–280. [CrossRef]
15. Giacomazzi, L.; Martin-Samos, L.; Boukenter, A.; Ouerdane, Y.; Girard, S.; Alessi, A.; de Gironcoli, S.; Richard, N. Photoactivated processes in optical fibers: Generation and conversion mechanisms of twofold coordinated Si and Ge atoms. *Nanotechnology* **2017**, *28*, 195202. [CrossRef] [PubMed]
16. Fujimaki, M.; Watanabe, T.; Katoh, T.; Kasahara, T.; Miyazaki, N.; Ohki, Y. Structures and generation mechanisms of paramagnetic centers and absorption bands responsible for Ge-doped SiO_2 optical-fiber gratings. *Phys. Rev. B* **1998**, *57*, 3920–3926. [CrossRef]
17. Tomashuk, A.L.; Salgansky, M.Y.; Kashaykin, P.F.; Khopin, V.F.; Sultangulova, A.I.; Nishchev, K.N.; Borisovsky, S.E.; Guryanov, A.N.; Dianov, E.M. Enhanced Radiation Resistance of Silica Optical Fibers Fabricated in High O_2 Excess Conditions. *J. Lightw. Technol.* **2014**, *32*, 213–219. [CrossRef]
18. Zotov, K.V.; Likhachev, M.E.; Tomashuk, A.L.; Bubnov, M.M.; Yashkov, M.V.; Guryanov, A.N.; Klyamkin, S.N. Radiation-Resistant Erbium-Doped Fiber for Spacecraft Applications. *IEEE Trans. Nucl. Sci.* **2008**, *55*, 2213–2215. [CrossRef]
19. Awazu, K.; Kawazoe, H.; Yamane, M. Simultaneous generation of optical absorption bands 5.14 and 0.452 eV in 9 SiO_2:GeO_2 glasses heated under H_2 atmosphere. *J. Appl. Phys.* **1990**, *68*, 2713–2718. [CrossRef]
20. Bradley, D.A.; Khandaker, M.U.; Alanazi, A. Irradiated glass and thermoluminescence yield: Dosimetric utility reviewed. *Radiat. Phys. Chem.* **2020**, *170*, 108680. [CrossRef]

21. Campanella, C.; Gutilla, A.; Morana, A.; De Michele, V.; Muller, C.; Aubry, M.; Mady, F.; Marin, E.; Ouerdane, Y.; Boukenter, A.; et al. Photobleaching Effect on Infrared Radiation-Induced Attenuation of Germanosilicate Optical Fibers at MGy Dose Levels. *IEEE Trans. Nucl. Sci.* **2021**, *68*, 1688–1693. [CrossRef]
22. Alessi, A.; Girard, S.; Reghioua, I.; Fanetti, M.; Di Francesca, D.; Agnello, S.; Cannas, M.; Marcandella, C.; Martin-Samos, L.; Richard, N.; et al. Gamma and *X*-ray irradiation effects on different Ge and Ge/F doped optical fibers. *J. Appl. Phys.* **2015**, *118*, 85901. [CrossRef]
23. Skuja, L. Isoelectronic series of twofold coordinated Si, Ge, and Sn atoms in glassy SiO_2: A luminescence study. *J. Non-Cryst. Solids* **1992**, *149*, 77–95. [CrossRef]
24. Reghioua, I.; Girard, S.; Alessi, A.; DiFrancesca, D.; Martin-Samos, L.; Fanetti, M.; Richard, N.; Raine, M.; Valant, M.; Boukenter, A.; et al. Cathodoluminescence investigation of Ge-point defects in silica-based optical fibers. *J. Lumin.* **2016**, *179*, 1–7. [CrossRef]
25. Simmons, H.W.; Nockolds, C.E.; Atkins, G.R.; Poole, S.B.; Sceats, M.G. Cathodoluminescence of defects in optical fibers and optical fiber preforms. *Electron. Lett.* **1992**, *27*, 1432–1433.
26. Alessi, A.; Girard, S.; Cannas, M.; Agnello, S.; Boukenter, A.; Ouerdane, Y. Evolution of Photo-induced defects in Ge-doped fiber/preform: Influence of the drawing. *Opt. Express* **2011**, *19*, 11680–11690. [CrossRef]
27. Raghavachari, K.; Pacchioni, G. Photoabsorption of dioxasilyrane and silanone groups at the surface of silica. *J. Chem. Phys.* **2001**, *114*, 4657–4662. [CrossRef]
28. Radzig, V.A. Reactive silica—A new concept of the structure of active sites. *Colloids Surf. A Physicochem.* **1993**, *74*, 91–100. [CrossRef]
29. Annenkov, V.V.; Danilovtseva, E.N.; Pal'shin, V.A.; Zelinskiy, S.N.; Chebykin, E.P.; Gak, V.Y.; Shendrik, R.Y. Luminescent siliceous materials based on sodium silicate, organic polymers and silicon analogs. *Mater. Chem. Phys.* **2017**, *185*, 65–72. [CrossRef]
30. Yoo, J.; Han, S.; Park, W.; Lee, T.; Park, Y.; Chang, H.; Kwang-Hahn, S.; Kwon, W. Defect-Induced Fluorescence of Silica Nanoparticles for Bioimaging Applications. *ACS Appl. Mater. Interfaces* **2018**, *10*, 44247–44256. [CrossRef]
31. Zyubin, A.S.; Mebel, A.M.; Lin, S.H. Photoluminescence of oxygen-containing surface defects in germanium oxides: A theoretical study. *J. Chem. Phys.* **2005**, *123*, 44701. [CrossRef]
32. Li, L.; Fukawa, T.; Matsuo, T.; Hashizume, D.; Fueno, H.; Tanaka, K.; Tamao, K. A stable germanone as the first isolated heavy ketone with a terminal oxygen atom. *Nat. Chem.* **2012**, *4*, 361–365. [CrossRef]
33. Kajihara, K.; Miura, T.; Kamioka, H.; Hirano, M.; Skuja, L.; Hosono, H. Surface Dissolution and Diffusion of Oxygen Molecules in SiO_2 Glass. *J. Ceram. Soc. Jpn.* **2004**, *112*, 559–562. [CrossRef]
34. Hoshino, T.; Hata, M.; Neya, S.; Nishioka, Y.; Watanabe, T.; Tatsumura, K.; Ohdomari, I. Diffusion of Molecular and Atomic Oxygen in Silicon Oxide. *Jpn. J. Appl. Phys.* **2003**, *42*, 3560–3565. [CrossRef]
35. Ixblue–Advanced Solutions for Navigation, Photonics and Maritime Autonomy. Available online: https://www.ixblue.com/ (accessed on 10 April 2022).
36. Di Francesca, D.; Agnello, S.; Girard, S.; Marcandella, C.; Paillet, P.; Boukenter, A.; Ouerdane, Y.; Gelardi, F.M. Influence of O_2-Loading Pretreatment on the Radiation Response of Pure and Fluorine-Doped Silica-Based Optical Fibers. *IEEE Trans. Nucl. Sci.* **2014**, *61*, 3302–3308. [CrossRef]
37. Di Francesca, D.; Girard, S.; Agnello, S.; Marcandella, C.; Paillet, P.; Boukenter, A.; Gelardi, F.M.; Ouerdane, Y. Near infrared radio-luminescence of O_2 loaded Rad-Hard silica optical fibers: A candidate dosimeter for harsh environments. *Appl. Phys. Lett.* **2014**, *105*, 183508. [CrossRef]
38. Raine, M.; Gaillardin, M.; Paillet, P. Geant4 physics processes for silicon microdosimetry simulation: Improvements and extension of the energy-range validity up to 10 GeV/nucleon. *Nucl. Instrum. Methods Phys. Res. B* **2014**, *325*, 97–100. [CrossRef]
39. Giannozzi, P.; Baroni, S.; Bonini, N.; Calandra, M.; Car, R.; Cavazzoni, C.; Ceresoli, D.; Chiarotti, G.L.; Cococcioni, M.; Dabo, I.; et al. QUANTUM ESPRESSO: A modular and open-source software project for quantum simulations of materials. *J. Phys. Condens. Matter* **2009**, *21*, 395502. [CrossRef]
40. Reghioua, I.; Girard, S.; Raine, M.; Alessi, A.; DiFrancesca, D.; Fanetti, M.; Martin-Samos, L.; Richard, N.; Valant, M.; Boukenter, A.; et al. Cathodoluminescence Characterization of Point Defects in Optical Fibers. *IEEE Trans. Nucl. Sci.* **2017**, *64*, 2318–2324. [CrossRef]
41. Reghioua, I.; Girard, S.; Alessi, A.; DiFrancesca, D.; Marin, E.; Morana, A.; Fanetti, M.; Martin-Samos, L.; Richard, N.; Raine, M.; et al. Study of point defects in as-drown and irradiated Ge-doped optical fibers using cathodoluminescence. *IOP Conf. Ser. Mater. Sci. Eng.* **2017**, *169*, 12006. [CrossRef]
42. Giacomazzi, L.; Umari, P.; Pasquarello, A. Vibrational spectra of vitreous germania from first-principles. *Phys. Rev. B* **2006**, *74*, 155208. [CrossRef]
43. Hamann, D.R. Diffusion of atomic oxygen in SiO_2. *Phys. Rev. Lett.* **1998**, *81*, 3447. [CrossRef]
44. Bongiorno, A.; Pasquarello, A. Multiscale modeling of oxygen diffusion through the oxide during silicon oxidation. *Phys. Rev. B* **2004**, *70*, 195312. [CrossRef]
45. Winkler, B.; Martin-Samos, L.; Richard, N.; Giacomazzi, L.; Alessi, A.; Girard, S.; Boukenter, A.; Ouerdane, Y.; Valant, M. Correlations between Structural and Optical Properties of Peroxy Bridges from First Principles. *J. Phys. Chem. C* **2017**, *121*, 4002–4010. [CrossRef]
46. Krasheninnikov, A.V.; Nordlund, K. Ion and Electron irradiation-induced effects in nanostructured materials. *J. Appl. Phys.* **2010**, *107*, 71301. [CrossRef]

47. Takeguchi, M.; Furuya, K.; Yoshihara, K. Electron energy loss spectroscopy study of the formation process of Si nanocrystals in SiO_2 due to electron stimulated desorption-decomposition. *Micron* **1999**, *30*, 147–150. [CrossRef]
48. Yakabe, T.; Fujita, D.; Yoshihara, K. Electron irradiation effect on depth profiling of a SiO_2/Si (1 0 0) surface by Auger electron spectroscopy. *Appl. Surf. Sci.* **2005**, *241*, 127–130. [CrossRef]
49. Kajihara, K.; Skuja, L.; Hosono, H. Diffusion and Reactions of Photoinduced Interstitial Oxygen Atoms in Amorphous SiO_2 Impregnated with ^{18}O-Labeled Interstitial Oxygen Molecules. *J. Phys. Chem. C* **2014**, *118*, 4282–4286. [CrossRef]